

The equatorial Indian Ocean upper water-column structure influenced by cross-basinal water exchange over the last ~40000 years

Ramanand Yadav^{1,2}, Sushant S. Naik^{1,2,*}, Jayu Narvekar^{1,2}

¹ CSIR-National Institute of Oceanography, Dona Paula, Goa-403004, India

² Academy of Scientific and Innovative Research (AcSIR), Ghaziabad-201002, India

*Corresponding author E-mail address: sushant@nio.org

Abstract

The central equatorial Indian Ocean (CEIO) is influenced by both, summer and winter monsoon and is known for cross basin exchange of water between the Arabian Sea (AS) and the Bay of Bengal (BoB). Here, we present planktic foraminiferal assemblage record from a sediment core (SSD-044/GC-01, 5°N; 77°E) from the CEIO, which is in the pathway of this cross-basin water exchange, in order to reconstruct changes in upper water column structure during the last 43 ka, at millennial year timescales. Our data displays an increase in ratio of mixed layer eutrophic to mixed layer oligotrophic foraminifer species from MIS (Marine Isotope Stage) 3 to MIS 2 which further decreased sharply during the last deglaciation and remained low thereafter. This trend matches well with the sedimentary C_{org} content which is interpreted as a productivity signal, in line with other studies from this region. Furthermore, the relative abundance of thermocline foraminifer species displayed highest values during MIS 3, a decrease through the MIS 2, a sharp decrease through the early deglaciation and an increase thereafter into the Holocene. Our records suggest that the increased productivity at this site seems to be fed by nutrient injection from nutricline to the photic zone which manifests in a corresponding increase in thermocline foraminifera species. The nutrient injection to the photic zone maybe a result of increased vertical/convective mixing due to increased flow of cooler/ high-salinity BoB water probably caused by decreased freshening of the BoB during glacials. Furthermore, our data suggests a warm, stratified upper water column and low surface nutrient (oligotrophic) conditions during the last deglaciation and the Holocene.

Keywords

Central equatorial Indian Ocean; Planktic foraminifera assemblage; Last glacial maximum; Winter monsoon; Productivity

Introduction

Monsoon derived rainfall is one of the most spectacular and dramatic phenomena over the Indian subcontinent/South Asian region (Pushpanjali et al., 2013). Indian agriculture depends on rainfall induced by the monsoon, the failure of which would adversely affect the food production as well as the country's economy (Gadgil, 2003). The South Asian/Indian monsoon system has its two climatic components, the southwest (SW)/summer monsoon and the northeast (NE)/winter monsoon. Between the months of June and September (SW monsoon), stronger winds lead to widespread upwelling, which brings cold, subsurface nutrient-rich water to the surface, which raises surface productivity in the western and northern Arabian Sea (AS) (Reichart et al., 1998). In contrast, the Bay of Bengal (BoB) receives huge amount of rainfall and fluvial discharge from the Ganga-Brahmaputra riverine system (Unger et al., 2003) and displays thermal stratification due to low sea surface salinity (SSS) associated with high sea surface temperatures (SST). In addition, the BoB exhibits very low surface productivity condition even though the nutrient availability is very high (Thushara and Vinayachandran, 2016). During November to February (NE monsoon), cold and dry winds enhance convective mixing in the northeastern AS making it one of most productive regions of the World Ocean (Banse and McClain, 1986; Madhupratap et al., 1996; Prasanna Kumar and Narvekar, 2005). In contrast, the BoB surface productivity moderately increases, especially in the northern BoB, due to winter monsoon wind induced cooling (Stoll et al., 2007).

Water circulation at the southern tip of the Indian peninsula experiences seasonal changes, a low saline-water current from the BoB in winter monsoon whereas in summer monsoon the current reverses and brings in high salinity water from the Arabian Sea at depths of 0 to 100m. This region experiences upwelling during the summer monsoon, leading to high productivity in this region (Levy et al., 2007). However, upwelling ceases towards the south and productivity then is not related to upwelling but to deepening of the mixed layer depth (Schulte et al., 1999). In the central equatorial Indian Ocean (CEIO), winds are weak nearer the equator during SW and NE monsoons, while high winds occur in this region during monsoon transition periods (Shaji and Ruma, 2020) and surface productivity conditions are circulation induced (Strutton et al., 2015). Monsoon reconstructions from the northern Indian Ocean suggest that the SW monsoon weakened and NE monsoon intensified during glacial periods (Prell et al., 1980; Cullen, 1981; Duplessy, 1982; Fontugne and Duplessey, 1986). The southeastern AS/ equatorial Indian Ocean is not studied much in terms of understanding productivity changes during the glacial-interglacial periods (Beaufort et al., 1997; Rostek et al., 1997; Cayre et al., 1999; Schulte et al., 1999; De et al., 2010; Gupta et al., 2010; Chandana et al., 2017; Mungekar et al., 2020). The above mentioned studies are spatially located ~5 degree latitude apart and within a water

depth difference of 500 m but show a great degree of difference in the OC preservation/accumulation. Therefore, this region is unique in terms of productivity variations. Our study aims to understand the upper water column structure and productivity variations in this region under the influence of shifting NE to SW monsoon conditions. We utilise foraminiferal indices from a sediment core (SSD-44/GC-01, 5°N and 77°E; water depth = 3160m; Fig. 1) from the CEIO which is influenced by the reversing monsoonal circulation and hence waters from the AS and BoB.

Regional Oceanography

Surface ocean circulation in the CEIO is driven by both summer as well as winter monsoon (Shankar et al., 2002). Between June and September, strong summer monsoon winds prevail over the AS and help the development of clockwise and anticyclonic circulation in the AS (Schott, 1983). The eastern branch of anticyclonic circulation forms the WICC and flows equatorward to join the Summer Monsoon Current (SMC) near the equatorial Indian Ocean (southeast AS) region (Shetye et al., 1991). During the summer monsoon season, site SSD-044/GC-01 is influenced by the Arabian Sea High-Salinity Water (ASHSW) carried by the WICC (Prasanna Kumar et al., 2004). The study region is moderately productive as compared to other high productive regions like the southwest AS and the northeast AS (Schulte et al., 1999) and modern productivity conditions in this region are highest during the SW monsoon (Fig. 1d). Upwelling conditions are not so well marked at the site due to local precipitation during summer monsoon and moderately upwelled water is generally overlain by low saline water (Schulte et al., 1999). During the southwest monsoon and intermonsoon the thermocline as well as 0.5 μmol nitrate depth is shallow, which brings nutrient rich sub-surface/nutricline water into the mixed layer (Fig. 1). The mixed layer depth (MLD) does not vary much but remains slightly deeper during the SW monsoon. During the winter monsoon, as the wind system reverses, the EICC forms in the north-western BoB and flows equatorward to join the Winter Monsoon Current (WMC), south of Sri Lanka. During the winter monsoon, this region is influenced by low saline water from the BoB carried by the EICC (Schott and McCreary, 2001). The thermocline as well as 0.5 μmol nitrate depth are deeper during the winter monsoon (Fig. 1c and d).

Materials and methods

The gravity core SSD-044/GC-01 was recovered during RV Sindhu Sadhana cruise 44, from the eastern flank of Comorin Ridge (5°N and 77°E, water depth = 3160 m) from the CEIO. The core location is ~400 km away from southern tip of India (off Kanyakumari) and represents an open ocean regime (Fig.1a and b).

The age model of the core was obtained using four AMS (accelerator mass spectrometry) ^{14}C dates on ~15mg of mixed planktic foraminiferal species, viz, *Globigerinoides ruber*, *Globigerinoides sacculifer*, *Neogloboquadrina dutertrei* and *Globorotalia menardii*. Radiocarbon dating was carried out using the accelerator mass spectrometer facility at the University of Arizona, USA. The radiocarbon dates were calibrated to calendar ages using the calib 7.1 programme (Reimer et al., 2013) (See Table 1; Fig. 2).

In total, 75 samples from the top 1.5 m section of core were analysed for planktic foraminifer assemblages. An appropriate portion of sediments was oven dried at 50°C, weighed and soaked in distilled water for 24 hrs. The soaked sediment were sieved through a 63 μm wet sieve. The coarse fraction (>63 μm) was dried, weighed and transferred into plastic vials. A portion of coarse fraction was dry-sieved through a 125 μm sieve. The >125 μm fraction was split several times and spread on a tray for picking foraminifera for census counts. A stereozoom microscope (MEIJI-EMZ 5TR) was used and a minimum of ~300 intact tests were picked for every sample. Based on census counts, the relative abundance of species was estimated in per gram dry sediment of >125 μm fraction. For species identification of planktic foraminifera, taxonomic concept of Kennett and Srinivasan (1983) and Hemleben et al. (1989) were followed.

Finely ground sediment samples were used for the analysis of total and inorganic carbon. Inorganic carbon (IC) content was determined with a coulometer (UIC, Inc-CM140 acidification module). Analytical grade calcium carbonate was used as a standard reference material. The precision of measurements were better than $\pm 2\%$. Total carbon (TC) was measured on a Shimadzu-Total Organic Carbon Analyzer; Model: TOC LCPH. The results have a precision within $\pm 3\%$ as obtained for NC soil standard. Wt. % of OC (organic carbon) was calculated as the difference between TC and IC.

Results

The coarse fraction mainly comprised biogenic remains and varied from 8 to 28 % throughout the 43 ka period. It was <21% in most samples and showed an increase after ~15 ka with the highest value of 30% at ~5.5 ka, in the Holocene (Fig.3A). Planktic foraminifera *Neogloboquadrina dutertrei* and *Globigerinita glutinata* were the most abundant species in the planktic foraminiferal assemblage. Other dominant species include *Globigerinoides ruber*, *Globigerinoides sacculifer*, *Globorotalia menardii* and *Pulleniatina obliquiloculata*. *Globigerina bulloides* was the least abundant species out of the seven planktic foraminifera species. A lower abundance of *G. ruber* was observed during the Last Glacial Maximum (LGM) and later part of the Holocene, while a higher abundance of *G. ruber* was observed between ~19ka and ~9ka. The relative abundance of *G. sacculifer* was low from ~43ka

to ~19ka, and was high during the Holocene. The lowest and highest abundance of *G. sacculifer* was seen at ~40ka and ~7ka, respectively. The relative abundance of *G. glutinata* was high between 43ka and 21ka, and low between ~21ka and ~3 ka, except at ~14ka. Globigerinoides *sacculifer* showed an opposite pattern to that of *G. glutinata*, throughout the 43 ka. The lowest and highest abundances of *G. glutinata* were seen at ~8 ka and ~26ka, respectively. The relative abundance of *G. bulloides* was high during the LGM and showed relatively similar pattern to *G. glutinata* and *N. dutertrei* during the last 43 ka. *Neogloboquadrina dutertrei* was the second most dominant species out of seven planktic foraminifer species and its trend is comparable to that of *G. bulloides*. Relative abundance of *P. obliquiloculata* was highest at ~43 ka and remained so till ~ 26 ka after which it decreased to 23ka. *Pulleniatina obliquiloculata* showed an increase during the LGM, a decreasing trend from ~18.5ka to ~14 ka and a slight increase in the Holocene. Relative abundance of *G. menardii* showed a similar pattern to *N.dutertrei* during the last 43 ka, except during the late Holocene (Fig.3H). A continuous increase in the relative abundance of *G. menardii*, *G. bulloides*, *N. dutertrei*, *P. obliquiloculata*, *G. glutinata*, and *G. sacculifer* was observed during the Holocene. In contrast, relative abundance of *G. ruber* showed a decreasing trend during the Holocene epoch.

The ratio of relative abundance of mixed layer eutrophic species (MLES=*G.bulloides* and *G. glutinata*) to mixed layer oligotrophic species (MLOS= *G.ruber*, *G.sacculifer*, *G.quadrilobatus* and *G.triloba*) and relative abundance of thermocline species (*P. obliquiloculata*, *N. dutertrei*, *G. menardii* and *G. tumida*) is shown during the last 43 ka (Fig.4A, B). The MLOS represent low nutrient conditions, whereas MLES represent high nutrient conditions. Thus, the ratio of MLES to MLOS has implications for mixed layer nutrient conditions and surface productivity of this region (Satpathy et al., 2020). This ratio varied from 0.25 to 2.6 and was high during MIS 3, increased during MIS 2 and then decreased during MIS 1. The relative abundance of thermocline foraminifer species showed maximum values during MIS 3, a decrease through the MIS 2 and early deglaciation and an increase thereafter into the Holocene. Organic carbon (C_{org} %) content varied from 0.4 to 2% and was higher during MIS 3 and 2 compared to MIS 1. The C_{org} was highest during the LGM and thereafter showed a continuous decrease (Fig. 4C).

5. Discussion

5.1 Upper water column conditions related to seasonal current reversal from SW to NE monsoon

The *Globigerinoides ruber* is a surface dwelling (spinose) planktic foraminifer and flourishes in top 50 m of the upper water column (photic zone) in tropical to subtropical ocean within an optimum sea surface temperature (SST) of 21-28°C and an optimum sea surface salinity (SSS) of 34.5-36.0 psu

(Bé and Hutson, 1977). It is a symbiont bearing species associated with zooxanthellae (Zheng et al., 2005) and susceptible to dissolution due to delicate nature of its test (Berger, 1971). It commonly occurs in the warm mixed layer favouring oligotrophic conditions (Fairbanks et al., 1982). On the other hand, *G. sacculifer* flourishes in the shallow mixed layer of tropical and subtropical ocean within an optimum temperature of 27-30°C and an optimum SSS of 34.9 psu (Bé and Hutson, 1977). Both these species were observed to be lower in abundance during the 43 to 19 ka period, after which they increased. Though *G. sacculifer* increased through the Holocene, *G. ruber* decreased after ~ 15 ka. In the northern Indian Ocean, earlier studies suggest the larger impact of salinity on the distribution pattern of these two species if they were showing an opposite pattern to each other. *Globigerinoides sacculifer* is dominant in <36 psu and *G. ruber* abundant in the >36 psu waters of the tropics to subtropics (Bé and Hutson, 1977; Sears et al., 2012). Increased abundance of *G. sacculifer* and decreased abundance of *G. ruber* in this study suggest low SSS condition at this site during the Holocene (Fig.3C, B). An increase in relative abundance of *G. sacculifer* in low salinity environment indicates nutrient-poor and highly oligotrophic conditions (Bijma et al., 1990; Bijma and Hemleben, 1994; Sears et al., 2012) during the Holocene. This is further supported by lower abundance of *G. bulloides* and *G. glutinata* as compared to higher abundance of *G. sacculifer*. Based on comparative study of species abundance we suggest that the core site was influenced by warmer SST and oligotrophic condition during the Holocene.

Although *G. bulloides* is an important constituent of sub-polar waters, it is also associated with upwelled, cold, nutrient-rich surface water of the AS during the summer monsoon (Cullen and Prell, 1984; Naidu, 1990; Kroon et al., 1991; Anderson and Prell, 1993; Naidu and Malmegren, 1996; Gupta et al., 2003). *Globigerina bulloides* also flourishes during the winter monsoon, wind induced convective mixing and high surface productivity conditions (Singh et al., 2006, 2011, 2018). Conversely, *G. glutinata* is a cosmopolitan species occurring from tropical to Polar Regions, and in the tropical Indian Ocean, *G. glutinata* flourishes in low SST conditions (Naidu, 1993). It feeds upon diatoms and is considered to be linked with winter diatom bloom due to vertical mixing and injection of nutrients into the photic zone (Schulz et al., 2002). Though the type of food plays an important role in governing the abundance of foraminifera species, the copious presence of *G. glutinata* in the core record (except during the Holocene) and relatively lower abundance of *G. bulloides* are suggestive of winter convection as the dominant physical forcing. During the Holocene, the increasing trend of *G. bulloides* and decreasing trend of *G. glutinata* were observed and indicate the signal of summer monsoon intensification. An increase in relative abundance of *G. bulloides* in the Holocene epoch may be due to sporadically upwelled water in the southeastern Arabian Sea which may have influenced our

site through the WICC during strong SW monsoon. In contrast, decreasing trend in relative abundance of *G. glutinata* during the Holocene suggest that the NE monsoon signal was replaced by that of the SW monsoon.

Neogloboquadrina dutertrei is a thermocline dwelling species (Ravelo et al., 1990; Ravelo and Fairbank, 1992) and flourishes in high nutrient (eutrophic) conditions. In the tropical ocean, the abundance of *N. dutertrei* depends upon change in the thermocline depth (Andreasen and Ravelo, 1997; Jian et al., 2000) and also during enhanced surface primary productivity, when nutrients are (through vertical mixing/upwelling) brought in to the photic zone (Fairbanks et al., 1982; Schiebel et al., 2001). In the northern Indian Ocean, *N. dutertrei* abundance was low in the high upwelling region of the western AS compared to low saline region of the BoB (Cullen and Prell, 1984), which suggests that its abundance is not governed by upwelling but rather controlled by salinity. The abundance of *N. dutertrei* remained high from 43 ka to 21 ka and thereafter a gradual decrease except during the late Holocene. As our core location experiences influx of low saline waters derived from the BoB through the EICC (Wyrki, 1973), the intrusion of this nutrient-rich water into the photic zone by advection (Prasanna Kumar et al., 2004) may also increase the surface productivity in the study region. The temporal variation in abundance of *N. dutertrei* was correlated with surface salinity condition during glacial-interglacial periods associated with the strength of NE monsoon wind (Duplessy, 1982). We suggest that periods which show higher relative abundances of *N. dutertrei*, *G. glutinata* and *G. bulloides* represent cold glacial periods with high nutrients levels and less stratified surface water. Further, we also suggest that enhanced surface productivity during cold glacial intervals was triggered by the strengthening of the NE monsoon. Such a connection between the NE monsoon intensity, surface productivity (injection of nutrients through vertical mixing to photic zone) and sea surface hydrography was seen in the northern Indian Ocean on glacial-interglacial time scale during the late Quaternary period (Rostek et al., 1997; Reichert et al., 1998; Schulte et al., 1999; Schulte and Muller, 2001; Ivanova et al., 2003; Singh et al., 2006, 2011, 2018).

Pulleniatina obliquiloculata calcifies within the thermocline and is highly resistant to dissolution due to its thick walled test (Berger, 1970). Relative abundance of *P. obliquiloculata* was >5% in majority of the samples except a few samples in the upper section of the core which exhibit <5% abundance (Fig. 3G). Low abundance of *P. obliquiloculata* during the Younger Dryas (YD) suggests an abrupt weakening of the SW monsoon (Schulz et al., 1998). Increased abundance of *P. obliquiloculata* during LGM was slightly lower in comparison to MIS 3. This increased abundance does not reflect low-nutrient conditions as other nutrient-loving species like *N. dutertrei* and *G. glutinata* were higher during the LGM. The relative abundance of *G. menardii* showed an inconsistent

decreasing trend from 43 ka to 17 ka and a progressive increasing trend from ~ 17 ka, a pattern similar to *N.dutertrei*. *Globorotalia menardii* secretes its test at thermocline depths allied with high chlorophyll concentration (Sexton and Norris, 2011) and its abundance varies with change in intermediate water ventilation leading to oxygen level variation at thermocline depth (Singh et al., 2018). Higher abundance of *G. menardii* during the LGM suggests high nutrient condition and poor ventilation at thermocline depth. The abundance pattern of *G. menardii* during last deglacial period showed a sharp decline and interestingly at ~ 17 ka Heinrich Event 1 it was completely absent. The complete disappearance of *G. menardii* at ~ 17 ka (corresponds to H1) may be related to change in the ventilation of intermediate water associated with low productivity (Jung et al., 2010; Naidu et al., 2014; Singh et al., 2018).

5.2 Productivity variations related to upper water column hydrography

Here we present the change in hydrographic condition during key periods over last 43 ka based on combined mixed layer oligotrophic species (MLOS= *G.ruber*, *G.sacculifer*, *G.quadrilobatus* and *G.triloba*), mixed layer eutrophic species (MLES= *G.bulloides* and *G.glutinata*) and thermocline species (*P.obliquiloculata*, *N.dutertrei*, *G.menardii* and *G.tumida*) (Fig. 4A, B). Our faunal proxy records suggest three distinct regimes of change in upper water column structure and productivity variation during the LGM (~23-19 ka), last deglacial period (~19 to 12 ka) and the Holocene (~11.7-0) (Fig.4).

5.2a The Last Glacial Maximum (LGM)

The higher ratio of MLES to MLOS during the LGM suggests that the mixed layer depth increased and shows eutrophication in the study region (Fig. 4A). This, coupled with increased abundance of thermocline species suggests not only nutrient-rich conditions in the surface mixed layer but also in the thermocline. Increased abundance of *N.dutertrei* (Fig.3F) during the LGM support a nutrient rich thermocline as well as high surface productivity. Furthermore, the ratios and species abundances suggest that the thermocline was relatively deeper. Higher ratios of MLES to MLOS, as well as higher relative abundance of thermocline species were also observed during MIS 3 and 2 in comparison to MIS 1. However the vertical/convective mixing was probably more intense during the LGM. Higher productivity during the MIS 3 and 2, especially the LGM, is supported by high C_{org} content (Fig. 4C). Studies from the northern Indian Ocean show similar high surface productivity conditions (eutrophication) due to intensified winter monsoon induced vertical/convective mixing during the LGM (Naqvi et al., 1998; Anil Kumar et al., 2005; Banakar et al., 2005; Ivanochko et al., 2005; Dahl and Oppo, 2006; Singh et al., 2006, 2018; Anand et al., 2008). A few mechanism have been put forth

to explain the LGM productivity increase in the equatorial Indian Ocean. It was suggested that LGM productivity increased due to an increase in intensity of NE monsoon winds (Bassinot et al., 1994; Rostek et al., 1994, 1997). However this mechanism was turned down as it is believed that the NE monsoon wind do not affect the study latitude (Knox, 1987). A second mechanism suggests that the presence of low-level jets for a long period of time at equatorial latitudes could stimulate the productivity in these areas (Beaufort, 1996), but is not supported by sediment core data (Cayre et al., 1999). Another mechanism for increased LGM productivity in the equatorial Indian Ocean is linked to period of high intensity of zonal wind called Indian Ocean Equatorial Westerlies (IEW) or “Wyrтки Jets” (Wyrтки, 1973; Beaufort et al., 1997). More lately two mechanisms were suggested for the increased glacial equatorial Indian Ocean productivity, a combination of significantly intensified Wyrтки Jets enhancing the nutrient levels in the photic layer, and the increased input of soil-nutrients from Indian sub-continent by the intensified winter monsoons (Punyu et al., 2014). The increased MLES to MLOS ratios from Core SSD-044/GC-01 along with relative abundance of thermocline species suggests that the mechanism of nutrient entrainment to the photic zone at this site is due to vertical/convective mixing which erodes the nutricline and brings nutrient from deeper depths into the photic zone (Singh et al., 2018). The strong vertical mixing is probably a result of cooler, high-saline BoB water inflow into the study area caused by decreased freshening of the BoB (Mahesh and Banakar, 2014; Saraswat et al., 2019). It should be noted that CEIO productivity during the LGM was moderate in comparison to high productive regions like northeastern AS.

5.2b The last deglaciation and Holocene

The MLES to MLOS ratio declined sharply during the deglaciation suggesting a rapid and major shift from a cold-nutrient rich condition (eutrophication) to a nutrient-poor (oligotrophic) environment with relatively warm stratified surface water and a decreased mixed layer depth (Fig. 4A). Several studies based on different geochemical proxies from the northern Indian Ocean have reported similar findings that support our faunal proxy based finding during the last deglacial period (Singh et al., 2006, 2018; Anand et al., 2008; Naik et al., 2017). In the AS, several records suggest reduced surface productivity during early deglaciation due to a weaker SW monsoon (Sirocko et al., 1993, 2000; Cayre and Bard, 1999; Singh et al., 2006). The switch in severity of NE monsoon was contemporary with northern Hemisphere cold event H-1 (Bond and Lotti, 1995). During ~ 17 ka which corresponds to H-1, the ratio of MLES to MLOS and C_{org} content was low and the relative abundance of thermocline species was the lowest. The decrease abundance of thermocline species in this case may be due to lower availability of food. The faunal proxy record at core location suggests that reduction in productivity condition may be related to ventilation of intermediate water during H-1 (Ziegler et al., 2010). During

H-1 there probably was a shift from NE monsoon induced vertical mixing to SW monsoon induced stratified sea surface condition (Singh et al., 2018). Further, the MLES to MLOS ratios were low during the Holocene which suggests oligotrophic conditions dominated and productivity was low, which is supported by lower C_{org} content. The thermocline species show a gradual increase through the Holocene. Decreased ratio of MLES to MLOS (stratification) and increased abundance of thermocline species indicate decreased in mixed layer depth and shoaling of thermocline. The Holocene is a period of increasing SW monsoon strength (Sarkar et al., 2000) and greater transport of low saline BoB waters. In modern times, before arrival of the summer monsoon, stratification was observed due to inflow of low saline BoB waters (Shenoi et al., 1999). The low saline waters inhibit upwelling in the study region and hence the productivity is weaker (Fig. 1b and d). This low productivity condition during the Holocene has been reported to be a result of transport of BoB low saline water (Sirocko et al., 2000; Kessarkar and Rao, 2007). These records are also in line with development of stratified conditions during the Holocene, leading to reduced productivity in the eastern Arabian Sea (Cabarcos et al., 2014).

Conclusions

The planktic foraminiferal assemblage record in Core SSD-044/GC-01 from the central equatorial Indian Ocean were used to decipher variation in the upper water column structure during the last 43ka. Variation in individual species abundance (ecologically sensitive species), ratio of relative abundance of mixed layer (eutrophic and oligotrophic) species, thermocline species and C_{org} content were observed for change in productivity conditions in the study region. Faunal proxy and C_{org} content reveals that productivity was high during MIS 3 and 2, especially during the Last Glacial Maximum. The large increase in productivity during the Last Glacial Maximum was probably due to enhanced vertical mixing and entrainment of nutrient from nutracline to mixed layer. The higher abundance of *G. menardii* during the Last Glacial Maximum and late Holocene suggest that thermocline water at this site was poorly ventilated in comparison to the last deglaciation. There was a rapid decline in surface productivity and warm, stratified upper water column and low surface nutrient (oligotrophic) condition prevailed during the last deglaciation and the Holocene.

Acknowledgements

Authors are thankful to Director CSIR- National Institute of Oceanography, Goa, India for permission to publish this work. We thanks ship cell, NIO, captain and crew members of RV Sindhu Sadhana for their assistance during the cruise. This core was obtained as a part of the MoES project 'Biogeochemical Process and Paleoceanographic Studies of the Eastern Indian Ocean'. RY is thankful

to CSIR-Senior Research Fellow (SRF) with the Grant No.31/026(0291)/2016-EMR-I for providing the research fellowship. This is National Institute of Oceanography contribution XXXX

References

- Anand, P., Kroon, D., Singh, A.D., Ganeshram, R.S., Ganssen, G., Elderfield, H., 2008. Coupled sea surface temperature–seawater $\delta^{18}\text{O}$ reconstructions in the Arabian Sea at the millennial scale for the last 35 ka. *Paleoceanography* 23, PA4207. <https://doi.org/10.1029/2007PA001564>.
- Anderson, D.M., Prell, W.L., 1993. A 300 kyr record of upwelling off Oman during the late Quaternary: evidence of the Asian southwest monsoon. *Paleoceanography* 8, 193-208. <https://doi.org/10.1029/93PA00256>.
- Andreasen, D.J., Ravelo, A.C., 1997. Tropical Pacific Ocean thermocline depth reconstructions for the last glacial maximum. *Paleoceanography* 12, 395-413. <https://doi.org/10.1029/97PA00822>.
- Anil Kumar, A., Rao, V.P., Patil, S.K., Kessarkar, P.M., Thamban, M., 2005. Rock magnetic records of the sediments of the eastern Arabian Sea: Evidence for late Quaternary climatic change. *Mar. Geol.* 220, 59-82. <https://doi.org/10.1016/j.margeo.2005.06.038>.
- Banakar, V.K., Oba, T., Chodankar, A.R., Kuramoto, T., Yamamoto, M., Minagawa, M., 2005. Monsoon related changes in sea surface productivity and water column denitrification in the Eastern Arabian Sea during the last glacial cycle. *Mar. Geol.* 219, 99-108. <https://doi.org/10.1016/j.margeo.2005.05.004>.
- Banse, K., McClain, C.R., 1986. Winter blooms of phytoplankton in the Arabian Sea as observed by the Coastal Zone Color Scanner. *Mar. Ecol. Prog. Ser.* 34, 201-211. doi: <https://doi.org/10.3354/meps034201>.
- Bassinot, F.C., Labeyrie, L.D., Vincent, E., Quidelleur, X., Shackleton, N.J., Lancelot, Y., 1994. The astronomical theory of climate and the age of the Brunhes-Matuyama magnetic reversal. *Earth Planet. Sci. Lett.* 126, 91-108. [https://doi.org/10.1016/0012-821X\(94\)90244-5](https://doi.org/10.1016/0012-821X(94)90244-5).
- Bé, A.W.H., Hutson, W.H., 1977. Ecology of planktonic foraminifera and biogeographic patterns of life and fossil assemblages in the Indian Ocean. *Micropaleontology* 23, 369-414.
- Berger, W.H., 1970. Planktonic foraminifera: selective solution and the lysocline. *Mar. Geol.* 8, 111-138. [https://doi.org/10.1016/0025-3227\(70\)90001-0](https://doi.org/10.1016/0025-3227(70)90001-0).
- Berger, W.H., 1971. Sedimentation of planktonic foraminifera. *Mar. Geol.* 11, 325-358. [https://doi.org/10.1016/0025-3227\(71\)90035-1](https://doi.org/10.1016/0025-3227(71)90035-1).
- Beaufort, L., 1996. Dynamics of the monsoon in the equatorial Indian Ocean over the last 260,000 years. *Quat. Int.* 31, 13-18. [https://doi.org/10.1016/1040-6182\(95\)00017-D](https://doi.org/10.1016/1040-6182(95)00017-D).
- Beaufort, L., Lancelot, Y., Camberlin, P., Cayre, O., Vincent, E., Bassinot, F., Labeyrie, L., 1997. Insolation cycles as a major control of equatorial Indian Ocean primary productivity. *Science* 278, 1451–1454. <https://doi.org/10.1126/science.278.5342.1451>.

- Bijma, J., Hemleben, C., 1994. Population dynamics of the planktic foraminifer *Globigerinoides sacculifer* (Brady) from the central Red Sea. *Deep-sea Res. Part I* 41, 485-510. [https://doi.org/10.1016/0967-0637\(94\)90092-2](https://doi.org/10.1016/0967-0637(94)90092-2).
- Bijma, J., Faber, W.W., Hemleben, C., 1990. Temperature and salinity limits for growth and survival of some planktonic foraminifers in laboratory cultures. *J. Foramin. Res.* 20, 95-116. <https://doi.org/10.2113/gsjfr.20.2.95>.
- Bond, G.C., Lotti, R., 1995. Iceberg discharges into the North Atlantic on millennial time scales during the last glaciation. *Science* 267, 1005-1010. <https://doi.org/10.1126/science.267.5200.1005>.
- Cabarcos, E., Flores, J.A., Singh, A.D., Sierro, F.J., 2014. Monsoonal dynamics and evolution of the primary productivity in the eastern Arabian Sea over the past 30 ka. *Palaeogeogr. Palaeoclimatol. Palaeoecol.* 411, 249-256. <http://dx.doi.org/10.1016/j.palaeo.2014.07.006>.
- Cayre, O., Bard, E., 1999. Planktonic foraminiferal and alkenone records of the last deglaciation from the eastern Arabian Sea. *Quat. Res.* 52, 337-342. <https://doi.org/10.1006/qres.1999.2083>.
- Cayre, O., Beaufort, L., Vincent, E., 1999. Paleoproductivity in the Equatorial Indian Ocean for the last 260,000 yr: a transfer function based on planktonic foraminifera. *Quat. Sci. Rev.* 18, 839-857.
- Chandana, K.R., Bhushan, R., Jull, A.J.T., 2017. Evidence of poor bottom water ventilation during LGM in the equatorial Indian Ocean. *Front. Earth Sci.* 5(84), 1-10. <https://doi.org/10.3389/feart.2017.00084>.
- Cullen, J.L., 1981. Microfossil evidence for changing salinity patterns in the Bay of Bengal over the last 20000 years. *Palaeogeogr. Palaeoclimatol. Palaeoecol.* 35, 315-356. [https://doi.org/10.1016/0031-0182\(81\)90101-2](https://doi.org/10.1016/0031-0182(81)90101-2).
- Cullen, J.L., Prell, W.L., 1984. Planktonic foraminifera of the northern Indian Ocean: distribution and preservation in surface sediments. *Mar. Micropaleontol.* 9, 1-52. [https://doi.org/10.1016/0377-8398\(84\)90022-7](https://doi.org/10.1016/0377-8398(84)90022-7).
- Dahl, K.A., Oppo, D.W., 2006. Sea surface temperature pattern reconstructions in the Arabian Sea. *Paleoceanography* 21, PA1014. <https://doi.org/10.1029/2005PA001162>.
- De, S., Sarkar, S., Gupta, A.K., 2010. Orbital and suborbital variability in the equatorial Indian Ocean as recorded in sediments of the Maldives Ridge (ODP Hole 716A) during the past 444 ka. In: Clift, P.D., Tada, R., Zheng, H. (Eds.), *Geol. Soc. Lond. Spec. Publ.* 342, 17-27. <https://doi.org/10.1144/SP342.3>.
- Duplessy, J.C., 1982. Glacial to interglacial contrasts in the northern Indian Ocean. *Nature* 295, 494-498. <https://doi.org/10.1038/295494a0>.
- Fairbanks, R.G., Sverdlow, M., Free, R., Wiebe, P.H., Bé, A.W.H., 1982. Vertical distribution and isotopic fractionation of living planktonic foraminifera from the Panama Basin. *Nature* 298, 841-844. <https://doi.org/10.1038/298841a0>.

- Fontugne, M.R., Duplessy, J.C., 1986. Variations of the monsoon regime during the upper Quaternary: evidence from carbon isotopic record of organic matter in North Indian Ocean sediment cores. *Palaeogeogr. Palaeoclimatol. Palaeoecol.* 56, 69-88. [https://doi.org/10.1016/0031-0182\(86\)90108-2](https://doi.org/10.1016/0031-0182(86)90108-2).
- Gadgil, S., 2003. The Indian monsoon and its variability. *Annu. Rev. Earth Planet. Sci.* 31, 429-467. <https://doi.org/10.1146/annurev.earth.31.100901.141251>.
- Gupta, A.K., Anderson, D.M., Overpeck, J.T., 2003. Abrupt changes in the Asian southwest monsoon during the Holocene and their links to the North Atlantic Ocean. *Nature* 421, 354-357. <https://doi.org/10.1038/nature01340>.
- Gupta, A.K., Sarkar, S., De, S., Clemens, S.C., Velu, A., 2010. Mid-Brunhes strengthening of the Indian Ocean Dipole caused increased equatorial East African and decreased Australasian rainfall. *Geophys. Res. Lett.* 37, L06706. <http://dx.doi.org/10.1029/2009GL042225>.
- Hemleben, C., Spindler, M., Anderson, O.R., 1989. *Modern Planktonic Foraminifera*. Springer-Verlag, New York, pp. 363.
- Hemming, S.R., 2004. Heinrich events: Massive late Pleistocene detritus layers of the North Atlantic and their global climate imprint. *Rev. Geophys.* 42, RG1005. <https://doi.org/10.1029/2003RG000128>.
- Ivanochko, T.S., Ganeshram, R.S., Brummer, G.J.A., Ganssen, G., Jung, S.J.A., Moreton, S.G., Kroon, D., 2005. Variations in tropical convection as an amplifier of global climate change at the millennial scale. *Earth Planet. Sci. Lett.* 235, 302-314. <https://doi.org/10.1016/j.epsl.2005.04.002>.
- Ivanova, E., Schiebel, R., Singh, A.D., Schmiedl, G., Niebler, H.S., Hemleben, C., 2003. Primary production in the Arabian Sea during the last 135 000 years. *Palaeogeogr. Palaeoclimatol. Palaeoecol.* 197, 61-82. [https://doi.org/10.1016/S0031-0182\(03\)00386-9](https://doi.org/10.1016/S0031-0182(03)00386-9).
- Jian, Z., Wang, P., Chen, M.P., Li, B., Zhao, Q., Bühring, C., Laj, C., Lin, H.L., Pflaumann, U., Bian, Y., Wang, R., 2000. Foraminiferal responses to major Pleistocene paleoceanographic changes in the southern South China Sea. *Paleoceanography* 15, 229-243. <https://doi.org/10.1029/1999PA000431>.
- Jung, S.J.A., Kroon, D., Ganssen, G., Peeters, F., Ganeshram, R., 2010. Southern Hemisphere intermediate water formation and the bi-polar seesaw. *PAGES news* 18(1), 36-38. <https://doi.org/10.22498/pages.18.1.36>.
- Kennett, J.P., Srinivasan, M.S., 1983. *Neogene Planktonic Foraminifera, a Phylogenetic Atlas*. Hutchinson and Ross Publications, Pennsylvania, pp. 265.
- Kessarkar, P.M., Rao, V.P., 2007. Organic carbon in sediments of the southwestern margin of India: Influence of productivity and monsoon variability during the Late Quaternary. *J. Geol. Soc. India* 69, 42-52.
- Knox, R. A., 1987. The Indian Ocean: Interaction with the monsoon. In J. S. Fein & P. L. Stephens (Eds.), *Monsoons*, New York, Wiley, pp. 632.

- Kroon, D., Steens, T., Troelstra, S., 1991. Onset of monsoonal related upwelling in the western Arabian Sea. In: Prell, W.L., Niitsuma, N., et al. (Eds.), Proceedings of the ODP, Sci. Results 117, pp. 257–264.
- Lévy, M., Shankar, D., André, J.M., Shenoi, S.S.C., Durand, F., de Boyer Montégut, C., 2007. Basin-wide seasonal evolution of the Indian Ocean's phytoplankton blooms. *J. Geophys. Res.* 112, C12014. <https://doi.org/10.1029/2007JC004090>.
- Madhupratap, M., Kumar, S.P., Bhattathiri, P.M.A., Kumar, M.D., Raghukumar, S., Nair, K.K.C., Ramaiah, N., 1996. Mechanism of the biological response to winter cooling in the northeastern Arabian Sea. *Nature* 384, 549-552. <https://doi.org/10.1038/384549a0>.
- Mahesh, B.S., Banakar, V.K., 2014. Change in the intensity of low-salinity water inflow from the Bay of Bengal into the Eastern Arabian Sea from the Last Glacial Maximum to the Holocene: Implications for monsoon variations. *Palaeogeogr. Palaeoclimatol. Palaeoecol.* 397, 31-37. <https://doi.org/10.1016/j.palaeo.2013.05.024>.
- Mungekar, T.V., Naik, S.S., Nath, B.N., Pandey, D.K., 2020. Shell weights of foraminifera trace atmospheric CO₂ from the Miocene to Pleistocene in the central Equatorial Indian Ocean. *J. Earth. Syst. Sci.* 129, 1-9. <https://doi.org/10.1007/s12040-020-1348-6>.
- Naidu, P. D., 1990. Distribution of upwelling index planktonic foraminifera in the sediments of the western continental margin of India. *Oceanol. Acta.* 13, 327-333.
- Naidu, P.D., 1993. Distribution patterns of Recent planktonic foraminifera in surface sediments of the western continental margin of India. *Mar. Geol.* 110, 403-418. [https://doi.org/10.1016/0025-3227\(93\)90097-F](https://doi.org/10.1016/0025-3227(93)90097-F).
- Naidu, P.D., Malmgren, B.A., 1996. A high-resolution record of late Quaternary upwelling along the Oman Margin, Arabian Sea based on planktonic foraminifera. *Paleoceanography* 11, 129-140. <https://doi.org/10.1029/95PA03198>.
- Naidu, P.D., Singh, A.D., Ganeshram, R., Bharti, S.K., 2014. Abrupt climate-induced changes in carbonate burial in the Arabian Sea: Causes and consequences. *Geochem. Geophys. Geosyst.* 15, 1398-1406. <https://doi.org/10.1002/2013GC005065>.
- Naik, D.K., Saraswat, R., Lea, D.W., Kurtarkar, S.R., Mackensen, A., 2017. Last glacial-interglacial productivity and associated changes in the eastern Arabian Sea. *Palaeogeogr. Palaeoclimatol. Palaeoecol.* 483,147-156. <https://doi.org/10.1016/j.palaeo.2016.07.014>.
- Naqvi, S.W.A., Yoshinari, T., Jayakumar, D.A., Altabet, M.A., Narvekar, P.V., Devol, A.H., Brandes, J.A., Codispoti, L.A., 1998. Budgetary and biogeochemical implications of N₂O isotope signatures in the Arabian Sea. *Nature* 394, 462-464. <https://doi.org/10.1038/28828>.
- Prasanna Kumar, S., Narvekar, J., Kumar, A., Shaji, C., Anand, P., Sabu, P., Rijomon, G., Josia, J., Jayaraj, K.A., Radhika, A., Nair, K.K.C., 2004. Intrusion of the Bay of Bengal water into the Arabian Sea during winter monsoon and associated chemical and biological response. *Geophys. Res. Lett.* 31, L15304. <https://doi.org/10.1029/2004GL020247>.
- Prasanna Kumar, S., Narvekar, J., 2005. Seasonal variability of the mixed layer in the central Arabian Sea and its implication on nutrients and primary productivity. *Deep-Sea Res. Part II* 52, 1848-1861. <https://doi.org/10.1016/j.dsr2.2005.06.002>.

- Prell, W.L., Hutson, W.H., Williams, D.F., Bé, A.W., Geitzenauer, K., Molfino, B., 1980. Surface circulation of the Indian Ocean during the last glacial maximum, approximately 18,000 yr BP. *Quat. Res.* 14, 309-336. [https://doi.org/10.1016/0033-5894\(80\)90014-9](https://doi.org/10.1016/0033-5894(80)90014-9).
- Punyu, V.R., Banakar, V.K., Garg, A., 2014. Equatorial Indian Ocean productivity during the last 33 kyr and possible linkage to Westerly Jet variability. *Mar. Geol.* 348, 44-51. <https://doi.org/10.1016/j.margeo.2013.11.010>.
- Pushpanjali, B., Subrahmanyam, M. V., Murty, K.P.R.V., 2013. Findlater jet intensity and characteristics in relation to Indian summer monsoon. In: Leal M.D., Levins M.B.(Eds.), *Monsoons: Formation, Environmental Monitoring and Impact Assessment*, pp.47–63.
- Ravelo, A.C., Fairbanks, R.G., 1992. Oxygen isotopic composition of multiple species of planktonic foraminifera: Recorders of the modern photic zone temperature gradient. *Paleoceanography* 7, 815-831. <https://doi.org/10.1029/92PA02092>.
- Ravelo, A.C., Fairbanks, R.G., Philander, S.G.H., 1990. Reconstructing tropical Atlantic hydrography using planktonic foraminifera and an ocean model. *Paleoceanography* 5, 409-431. <https://doi.org/10.1029/PA005i003p00409>.
- Reichart, G.J., Lourens, L.J., Zachariasse, W.J., 1998. Temporal variability in the northern Arabian Sea oxygen minimum zone (OMZ) during the last 225,000 years. *Paleoceanography* 13, 607-621. <https://doi.org/10.1029/98PA02203>.
- Reimer, P.J., Bard, E., Bayliss, A., Beck, J.W., Blackwell, P.G., Ramsey, C.B., Buck, C.E., Cheng, H., Edwards, R.L., Friedrich, M., Grootes, P.M., 2013. IntCal13 and Marine13 radiocarbon age calibration curves 0–50,000 years cal BP. *Radiocarbon* 55, 1869-1887. https://doi.org/10.2458/azu_js_rc.55.16947.
- Rostek, F., Bard, E., Beaufort, L., Sonzogni, C., Ganssen, G., 1997. Sea surface temperature and productivity records for the past 240 kyr in the Arabian Sea. *Deep-Sea Res. Part II* 44, 1461-1480. [https://doi.org/10.1016/S0967-0645\(97\)00008-8](https://doi.org/10.1016/S0967-0645(97)00008-8).
- Rostek, F., Ruhland, G., Bassinot, F.C., Beaufort, L., Müller, P.J., Bard, E., 1994. Fluctuations of the Indian monsoon regime during the last 170,000 years: Evidence from sea surface temperature, salinity and organic carbon records. In *Global Precipitations and Climate Change*, Springer, Berlin, Heidelberg, pp. 27-51.
- Saraswat, R., Singh, D.P., Lea, D.W., Mackensen, A., Naik, D.K., 2019. Indonesian throughflow controlled the westward extent of the Indo-Pacific Warm Pool during glacial-interglacial intervals. *Global Planet. Change.* 183, 103031. <https://doi.org/10.1016/j.gloplacha.2019.103031>.
- Sarkar, A., Ramesh, R., B.L.K. Somayajulu, R. Agnihotri, A.J.T. Jull, G.S. Burr., 2000. High resolution Holocene monsoon record from the eastern Arabian Sea. *Earth Planet. Sci. Lett.* 177, 209-218. [https://doi.org/10.1016/S0012-821X\(00\)00053-4](https://doi.org/10.1016/S0012-821X(00)00053-4).
- Satpathy, R.K., Steinke, S., Singh, A.D., 2020. Monsoon-induced changes in surface hydrography of the eastern Arabian Sea during the early Pleistocene. *Geol. Mag.* 157, 1001-1011. <https://doi.org/10.1017/S0016756819000098>.

- Schiebel, R., Waniek, J., Bork, M., Hemleben, C., 2001. Planktic foraminiferal production stimulated by chlorophyll redistribution and entrainment of nutrients. *Deep-Sea Res. Part I* 48, 721-740. [https://doi.org/10.1016/S0967-0637\(00\)00065-0](https://doi.org/10.1016/S0967-0637(00)00065-0).
- Schott, F., 1983. Monsoon response of the Somali Current and associated upwelling. *Prog. Oceanogra.* 12, 357-381. [https://doi.org/10.1016/0079-6611\(83\)90014-9](https://doi.org/10.1016/0079-6611(83)90014-9).
- Schott, F.A., McCreary Jr, J.P., 2001. The monsoon circulation of the Indian Ocean. *Prog. Oceanogra.* 51, 1-123. [https://doi.org/10.1016/S0079-6611\(01\)00083-0](https://doi.org/10.1016/S0079-6611(01)00083-0).
- Schulte, S., Müller, P.J., 2001. Variations of sea surface temperature and primary productivity during Heinrich and Dansgaard-Oeschger events in the northeastern Arabian Sea. *Geo-Mar. Lett.* 21, 168-175. <https://doi.org/10.1007/s003670100080>.
- Schulte, S., Rostek, F., Bard, E., Rullkötter, J., Marchal, O., 1999. Variations of oxygen-minimum and primary productivity recorded in sediments of the Arabian Sea. *Earth Planet. Sci. Lett.* 173, 205-221. [https://doi.org/10.1016/S0012-821X\(99\)00232-0](https://doi.org/10.1016/S0012-821X(99)00232-0).
- Schulz, H., von Rad, U., Erlenkeuser, H., 1998. Correlation between Arabian Sea and Greenland climate oscillations of the past 110,000 years. *Nature* 393, 54-57. <https://doi.org/10.1038/31750>.
- Schulz, H., von Rad, U., Ittekkot, V., 2002. Planktic foraminifera, particle flux and oceanic productivity off Pakistan, NE Arabian Sea: modern analogues and application to the palaeoclimatic record. In: Clift, P.D., Kroon, D., Gaedicke, C., Craig, J. (Eds.), *Geol. Soc. Lond. Spec. Publ.* 195, 499–516. <https://doi.org/10.1144/GSL.SP.2002.195.01.27>.
- Seears, H.A., Darling, K.F., Wade, C.M., 2012. Ecological partitioning and diversity in tropical planktonic foraminifera. *BMC Evol. Biol.* 12, 54. <https://doi.org/10.1186/1471-2148-12-54>.
- Sexton, P.F., Norris, R.D., 2011. High latitude regulation of low latitude thermocline ventilation and planktic foraminifer populations across glacial–interglacial cycles. *Earth Planet. Sci. Lett.* 311, 69-81. <https://doi.org/10.1016/j.epsl.2011.08.044>.
- Shaji, C. and Ruma, S., 2020. On the seasonal and inter-annual variability of the equatorial Indian Ocean surface winds. *Meteorol. Atmospheric Phys.* 132, 353-376. <https://doi.org/10.1007/s00703-019-00690-9>.
- Shankar, D., Vinayachandran, P.N., Unnikrishnan, A.S., 2002. The monsoon currents in the north Indian Ocean. *Prog. Oceanogra.* 52, 63-120. [https://doi.org/10.1016/S0079-6611\(02\)00024-1](https://doi.org/10.1016/S0079-6611(02)00024-1).
- Shenoi, S.S.C., Shankar, D., Shetye, S.R., 1999. On the sea surface temperature high in the Lakshadweep Sea before the onset of the southwest monsoon. *J. Geophys. Res.* 104, 15703-15712. <https://doi.org/10.1029/1998JC900080>.
- Shetye, S.R., Gouveia, A.D., Shenoi, S.S.C., Michael, G.S., Sundar, D., Almeida, A.M., Santanam, K., 1991. The coastal current off western India during the northeast monsoon. *Deep-Sea Res.* 38, 1517-1529. [https://doi.org/10.1016/0198-0149\(91\)90087-V](https://doi.org/10.1016/0198-0149(91)90087-V).
- Singh, A.D., Kroon, D., Ganeshram, R.S., 2006. Millennial scale variations in productivity and OMZ intensity in the eastern Arabian Sea. *J. Geol. Soc. India* 68, 369-377.

- Singh, A.D., Jung, S.J., Darling, K., Ganeshram, R., Ivanochko, T., Kroon, D., 2011. Productivity collapses in the Arabian Sea during glacial cold phases. *Paleoceanography* 26, PA3210. <https://doi.org/10.1029/2009PA001923>.
- Singh, A.D., Jung, S.J., Anand, P., Kroon, D., Ganeshram, R.S., 2018. Rapid switch in monsoon-wind induced surface hydrographic conditions of the eastern Arabian Sea during the last deglaciation. *Quarter. Int.* 479, 3-11. <https://doi.org/10.1016/j.quaint.2018.03.027>.
- Sirocko, F., Sarnthein, M., Erlenkeuser, H., Lange, H., Arnold, M., Duplessy, J.C., 1993. Century-scale events in monsoonal climate over the past 24,000 years. *Nature* 364, 322-324. <https://doi.org/10.1038/364322a0>.
- Sirocko, F., Garbe-Schönberg, D., Devey, C., 2000. Processes controlling trace element geochemistry of Arabian Sea sediments during the last 25,000 years. *Global. Planet. Change.* 26, 217-303. [https://doi.org/10.1016/S0921-8181\(00\)00046-1](https://doi.org/10.1016/S0921-8181(00)00046-1).
- Stoll, H.M., Arevalos, A., Burke, A., Ziveri, P., Mortyn, G., Shimizu, N., Unger, D., 2007. Seasonal cycles in biogenic production and export in Northern Bay of Bengal sediment traps. *Deep Sea Res. Part II* 54, 558-580. <https://doi.org/10.1016/j.dsr2.2007.01.002>.
- Strutton, P.G., Coles, V.J., Hood, R.R., Matear, R.J., McPhaden, M.J., Phillips, H.E., 2015. Biogeochemical variability in the central equatorial Indian Ocean during the monsoon transition. *Biogeosciences* 12, 2367-2382. <https://doi.org/10.5194/bg-12-2367-2015>.
- Thushara, V., Vinayachandran, P.N., 2016. Formation of summer phytoplankton bloom in the northwestern Bay of Bengal in a coupled physical-ecosystem model. *J. Geophys. Res.* 121, 8535-8550. <https://doi.org/10.1002/2016JC011987>.
- Unger, D., Ittekkot, V., Schäfer, P., Tiemann, J., Reschke, S., 2003. Seasonality and interannual variability of particle fluxes to the deep Bay of Bengal: influence of riverine input and oceanographic processes. *Deep-Sea Res. Part II* 50, 897-923. [https://doi.org/10.1016/S0967-0645\(02\)00612-4](https://doi.org/10.1016/S0967-0645(02)00612-4).
- Wyrtki, K., 1973. Physical oceanography of the Indian ocean. In: Zeitzschel, B., Gerlach, S.A. (Eds.), *The Biology of the Indian Ocean*. Springer-Verlag, New York, pp. 18-36. https://doi.org/10.1007/978-3-642-65468-8_3.
- Zheng, F., Li, Q., Li, B., Chen, M., Tu, X., Tian, J., Jian, Z., 2005. A millennial scale planktonic foraminifer record of the mid-Pleistocene climate transition from the northern South China Sea. *Palaeogeogr., Palaeoclimatol., Palaeoecol.* 223, 349-363. <https://doi.org/10.1594/PANGAEA.694035>.
- Ziegler, M., Lourens, L.J., Tuenter, E., Hilgen, F., Reichert, G.J., Weber, N., 2010. Precession phasing offset between Indian summer monsoon and Arabian Sea productivity linked to changes in Atlantic overturning circulation. *Paleoceanography* 25, PA3213. <https://doi.org/10.1029/2009PA001884>.
- Zweng, M. M., J. R. Reagan, D. Seidov, T. P. Boyer, R. A. Locarnini, H. E. Garcia, A. V. Mishonov, O. K. Baranova, K. Weathers, C. R. Paver, and I. Smolyar, 2018. *World Ocean Atlas 2018, Volume 2: Salinity*. A. Mishonov Technical Ed.; NOAA Atlas NESDIS 82, 50 pp.

Legend to figures and table

- Figure: 1 Map showing the location of core SSD-044/GC-01 in the central equatorial Indian Ocean; (a) seasonal (summer) sea surface salinity (Zweng et al., 2018), (b) seasonal (winter) sea surface salinity overlain with geostrophic current velocity WICC: West Indian Coastal Current; EICC: East Indian Coastal Current; SMC: Southwest Monsoon Current; NMC: Northeast Monsoon Current (Schott and McCreary, 2001); (c) Monthly data of mixed layer depth (blue line) and depth of 0.5 μmol nitrate (redline), and (d) D20 thermocline depth (black line) and primary productivity (red line) calculated for the core site using World Ocean Atlas 2018 climatology.
- Figure: 2 Chronology of the core SSD-044/GC-01 established from 4 AMS radiocarbon dates (black filled symbols along with error bars), measured on mixed planktic foraminifera. The dates are plotted against the depth interval in the core and were used as tie points. Sedimentation rates between tie points are also shown.
- Figure: 3 Variation of ecologically sensitive planktic foraminifera species during the last 43ka. A. percentage of coarse fraction (CF) ($>63\mu\text{m}$); B-H, relative abundance of *G.ruber*, *G.sacculifer*, *G.glutinata*, *G.bulloides*, *N.dutertrei*, *P.obliquiloculata* and *G.menardii*. The shaded/dotted bars on plot indicate the timing and duration of the Younger Dryas (YD), Bølling Allerød (BA), Last Glacial Maximum (LGM), Heinrich events 1 to 4 (H-1,2,3,4) (Hemming, 2004). Marine isotope stages (MIS) 1, 2, 3 are also marked as arrows on top of the plot.
- Figure: 4 A. Ratio of mixed layer eutrophic species (MLES= *G.bulloides* and *G. glutinata*) to mixed layer oligotrophic species (MLOS= *G.ruber*, *G.sacculifer*, *G.quadrilobatus* and *G.triloba*) for the last 43ka. B. relative abundance of thermocline foraminifera (*P. obliquiloculata*, *N. dutertrei*, *G. menardii* and *G. tumida*) species C. Organic carbon content in sediment (bold lines in A and B show 3 point running averages)
- Table: 1 The details of Accelerator Mass Spectrometer (AMS) ^{14}C radiocarbon dates used to establish the chronology of the core SSD-044/GC-01

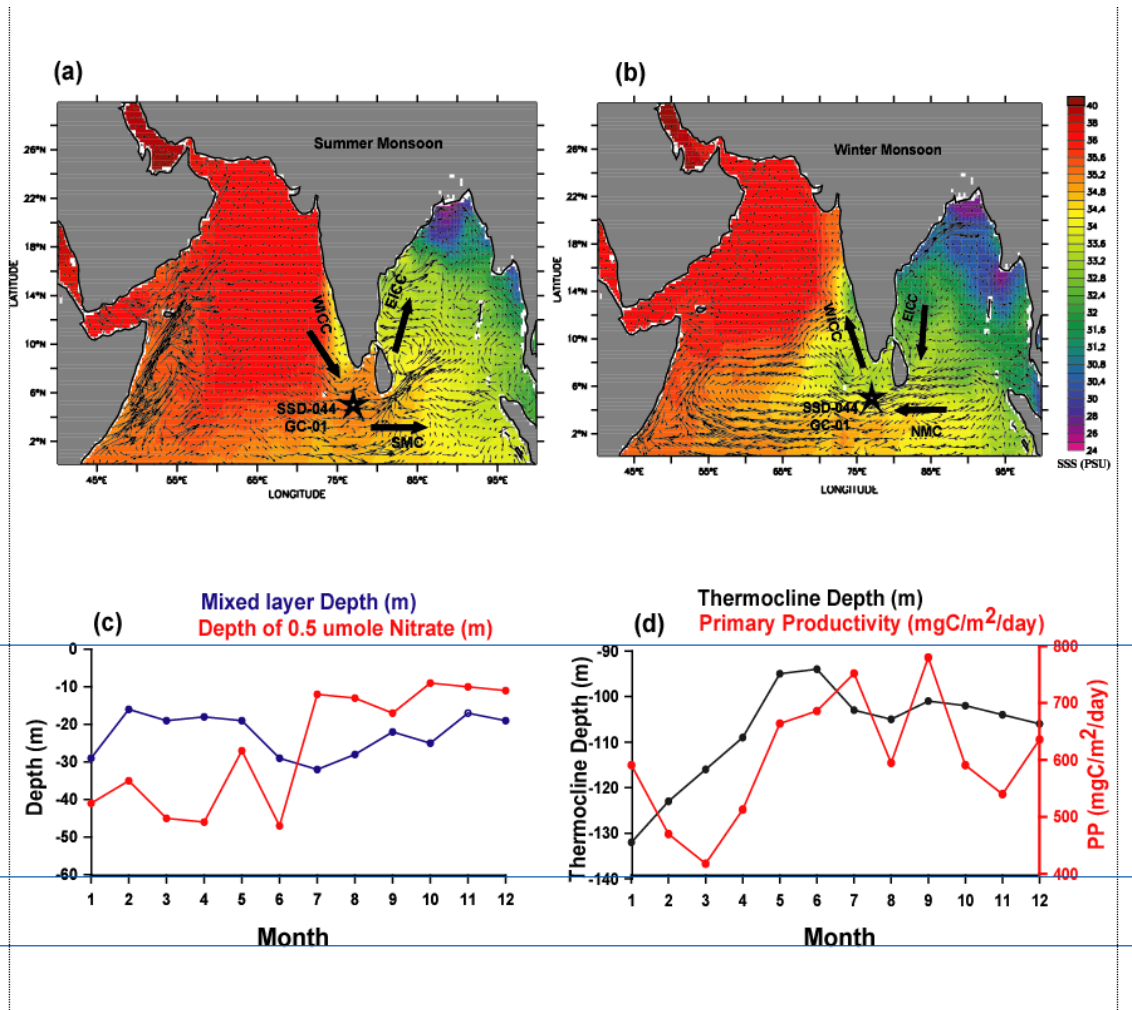


Figure 1

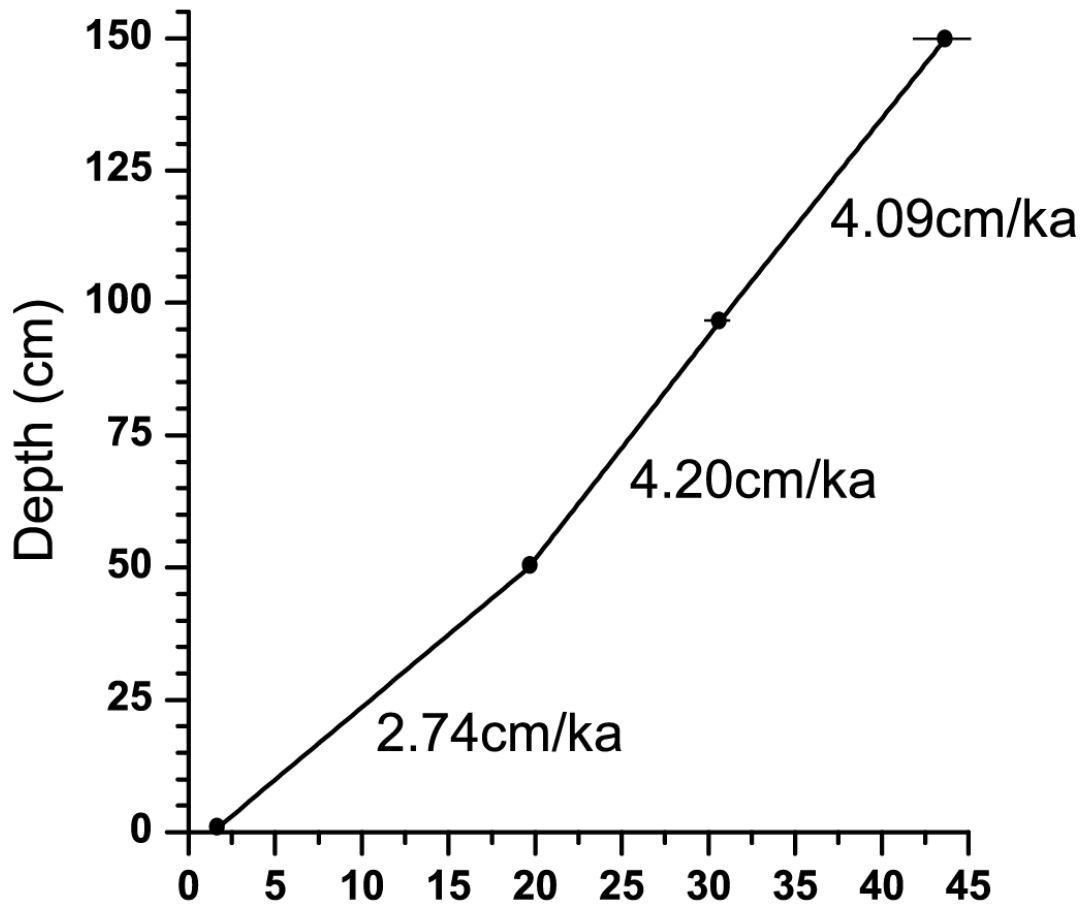


Figure 2

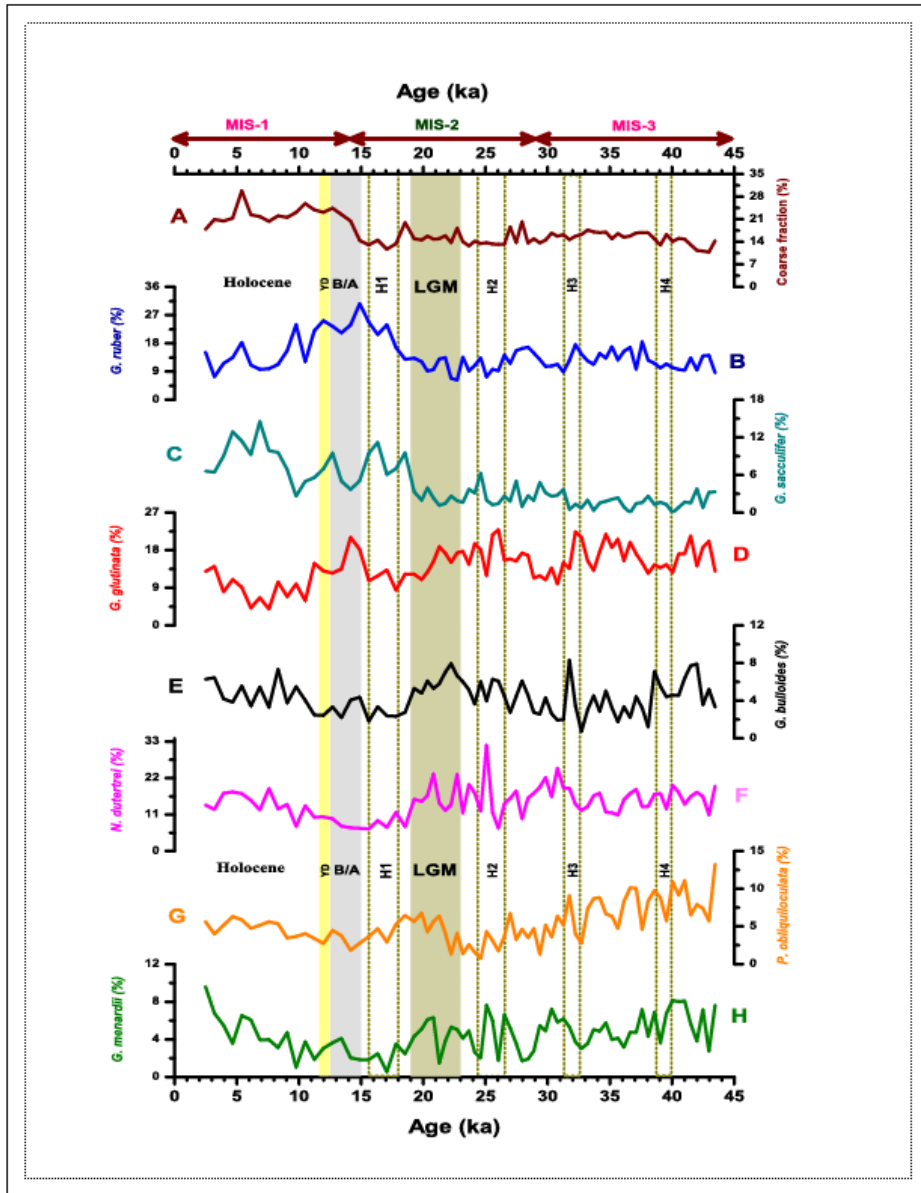


Figure 3

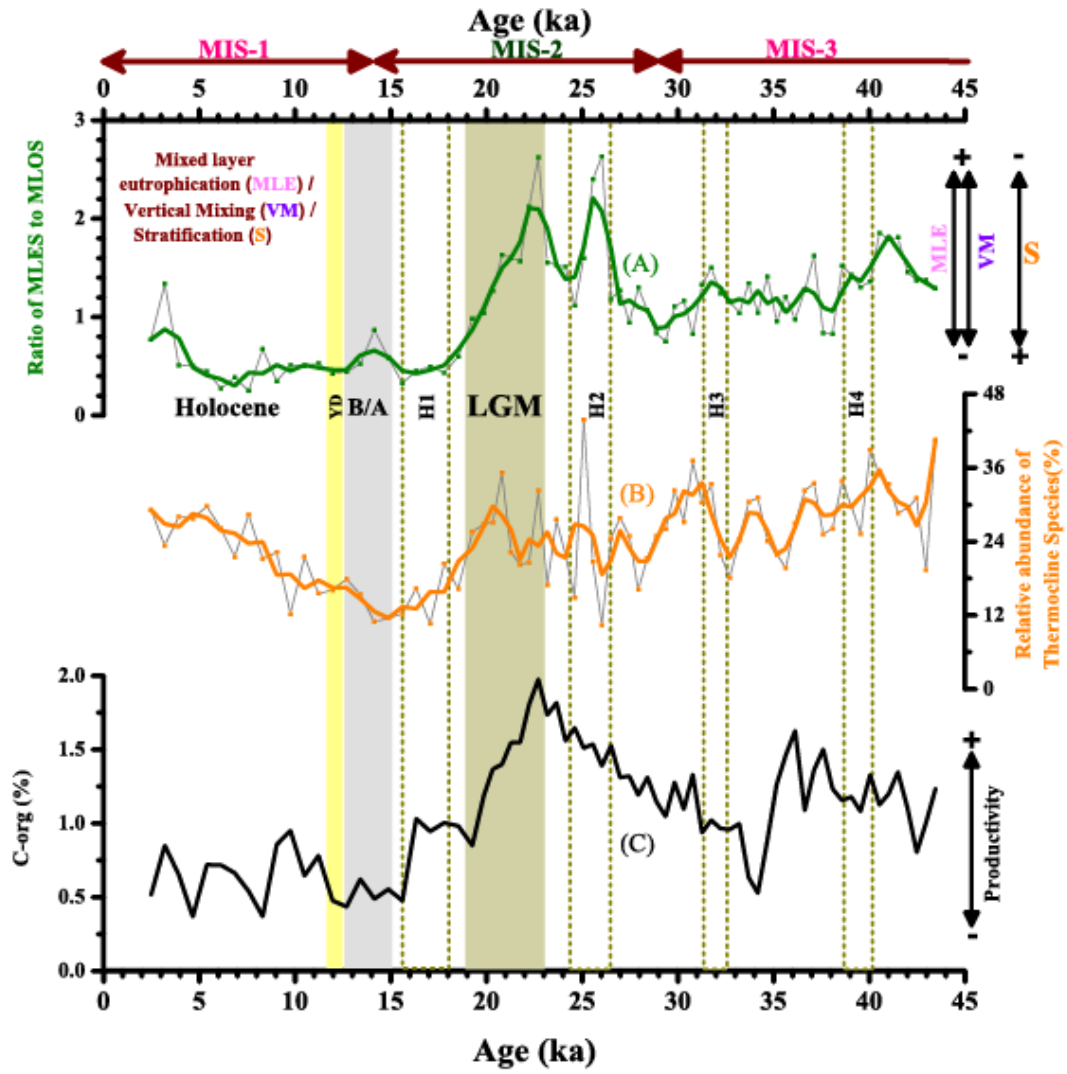


Figure 4

Table 1

S.No.	Depth (cm)	¹⁴ C age	¹⁴ C age error (±)	Calendar Years BP
1	1	2195	22	1748
2	50	16700	64	19624
3	100	28160	270	31504
4	150	40400	1200	43703